IEEE Access
Multidisciplinary | Rapid Review | Open Access Journal

Received 10 December 2023, accepted 19 December 2023, date of publication 5 January 2024,
date of current version 16 January 2024.

Digital Object Identifier 10.1109/ACCESS.2024.3350269

RESEARCH ARTICLE

A Novel Improved Grey Wolf Algorithm Based Global Maximum Power Point Tracker Method Considering Partial Shading

HASAN GUNDOGDU[1], ALPASLAN DEMIRCI[1], SAID MIRZA TERCAN[1], AND UMIT CALI[2,3], (Senior Member, IEEE)

[1]Department of Electrical Engineering, Yildiz Technical University, 34220 İstanbul, Turkey
[2]Department of Electric Energy, Norwegian University of Science and Technology, 7491 Trondheim, Norway
[3]School of Physics, Engineering and Technology, University of York, YO10 5DD York, U.K.

Corresponding author: Umit Cali (umit.cali@ntnu.no)

ABSTRACT Considering photovoltaic systems' sustainability and environmental friendliness, they have been widely used due to ease of installation as their cost reduces and their efficiency is improved. Analytical maximum power point tracking methods for photovoltaic system work effectively under uniform weather conditions. However, they may fall into local maximum power points due to partial shading conditions. Although numerous meta-heuristic methods can overcome these challenges, they can still be improved regarding the convergence time to the global maximum power point. This paper suggests an improved grey wolf optimization method to track global maximum power points, enhancing the convergence process and efficiency under various weather conditions. The proposed method has been verified experimentally under dynamic and real weather conditions, consisting of uniform and non-uniform weather conditions. The method provides better dynamic tracking speed and efficiency up to 82% and 1.4% compared to the basic grey wolf optimization. According to the daily performance evaluation, the IGWO reduces the runtime by up to 76% and improves energy harvesting up to 2.3% compared to basic grey wolf optimization. The obtained results validate the superiority of the method compared under partial shading conditions in terms of tracking time and accuracy.

INDEX TERMS Heuristic algorithms, improved grey wolf optimization, maximum power point tracking, partial shading, photovoltaic.

I. INTRODUCTION

The significant increase in energy demand, the recent environmental concerns, and the reserve problem of fossil fuels have led to a tendency towards renewable energy sources (RES). Solar photovoltaic (PV) energy generation is intermittent and variable because of sudden changes in irradiation and temperature. Maximizing efficiency under variable irradiance is a challenging issue for PV systems. Especially, partial shading due to cloud movements or improper positioning reduces the efficiency and output power. The maximum power point tracker (MPPT) keeps the PV array continuously on MPP with the help of optimization algorithms [1]. The non-linear nature of PV leads to many local maxima on characteristics curves under partial shading [2], [3]. There is only one MPP on the characteristic curve under uniform irradiance, as indicated by the red line in Figure 1. However, some local MPPs are on blue and green lines in Figure 1 due to partial shading. Besides, classical algorithms such as incremental conductance/resistance, perturb&observe (P&O) are insufficient to track the global MPP under non-uniform irradiance [4], [5], [6]. Therefore, several methodologies have also been proposed to determine the step size of analytical methods for reducing steady-state oscillations and maintaining a good tracking speed [7], [8].

Numerous studies have been conducted to track global MPP (GMPP) under partial shading conditions for reducing tracking time, power losses, and oscillations, enhancing

The associate editor coordinating the review of this manuscript and approving it for publication was Mostafa M. Fouda.

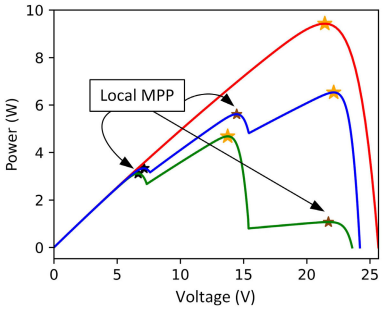

FIGURE 1. Maximum power points on the P-V curve (red: uniform, blue and green: non-uniform).

efficiency using various meta-heuristic optimization algorithms [9], [10]. It is required that they avoid falling into local maximum, especially under partial shading conditions, and can easily be implemented. Particle Swarm Optimization (PSO) is a bio-inspired, intelligence-based meta-heuristic optimization algorithm [11]. The PSO technique performs better than the conventional MPPT methods, which cannot track GMPP under partial shading conditions [12]. PSO has been extensively used for various engineering applications due to good accuracy, simpler structure, high adaptability, and few tuning parameters. Still, it has several drawbacks like steady-state oscillation, convergence ability, and tracking speed. Therefore, improving PSO in terms of searching speed and reducing oscillation have gained enormous attention from researchers [13], [14]. Harris Hawks optimization (HHO) is proposed by Heidari et al. [15], [16]. HHO has been utilized recently for multiple engineering problems like an MPPT algorithm to find the global MPP of PV array during partial shading (PS). The advantages of HHO for MPPT are effectively minimizing the undesired steady-state oscillation and high-power conversion efficiency with good accuracy. However, HHO may fall into local maximum points, and it takes longer to find the MPP under the shading conditions. Grey Wolf Optimization (GWO) is a recently emerged bio-inspired swarm-based meta-heuristic optimization algorithm introduced by Mirjalili et al. in 2014 [17]. The GWO gives competitive results compared to popular swarm-based algorithms in terms of accuracy, convergence independency, simple controlling, and the ability to deal with local minima. GWO is used to estimate unknown parameters of solar photovoltaics, such as series resistance, shunt resistance, and ideality factor [18], and to improve the efficiency of MPPT systems [19]. However, the accuracy and tracking time in the basic GWO can still be further improved for various partial shading conditions [20], [21].

Moreover, premature convergence and trapping into local optima prevent basic meta-heuristic algorithms from obtaining global maximum power points of PV array and lead power oscillations due to solar irradiation variations. Therefore, several researchers have tended to improve basic meta-heuristic algorithms to overcome these deficits [22]. The meta-heuristic algorithms control the swarm movements using several velocity-updating methods. For example, adding an inertia weight factor to the velocity equation can balance between the global and the local search. Furthermore, chaotic search, which is aperiodic motion, can eliminate disadvantages like premature convergence and trapping into local optima, improving the uniformity and ergodicity of the swarm [23]. For example, premature convergence can be overcome using a chaotic strategy assigning the individual position of the bat algorithm [24], [25]. The complex traditional MPPT techniques show poor performance in locating the global MPP under partial shading conditions [26], [27], [28]. Recently, there have been efforts to combine traditional MPPT methods with meta-heuristic algorithms to track global MPP under partial shading effectively [29]. Although hybridization has improved the MPPT performance, it has some disadvantages, such as increased complexity and computational burden [30], [31]. The proposed hybrid GWO with the Nelder-mead algorithm enhances the convergence rate. It decreases response time, avoiding unnecessary particle exploration and effectively reducing steady-state oscillations, especially under non-uniform weather conditions [32].

According to GWO, a new position for each wolf is created for the three leader wolves resulting in slower convergence, loss of diversity, and falling into the local optima. Sharing the hunting information between neighbor wolves can boost the search speed and avoid slipping into the local optimum [33], [34]. GWO has been modified to update only unequal duty values in any iterations to avoid unnecessary searches and long tracking times [35]. On the other hand, the linearly decreasing convergence parameter "a" cannot truly reflect the actual search process. If a non-linearly decreasing parameter was chosen, better convergence performance would be achieved with less tracking time and fewer iterations [36], [37]. For example, the cosine control parameter synchronously updates the positions further to enhance the global exploration capability [38]. Also, the improved GWO algorithm addressing the lack of population variety, premature convergence, and mismatch between exploitation and exploration has been implemented to tune the controller's gains of plug-in hybrid electric vehicles for efficient charging management [39]. Additionally, "a" is reduced at the early stage of the optimization process to maintain a faster convergence rate and increased at the later stage to expand the optimization range and avoid falling into the local optimum [40]. The proposed method using a non-linear tangent trigonometric function as a convergence factor has improved efficiency to 98.54% under various partial shading conditions with tracking time up to 0.24 s [41]. Additionally, an enhanced GWO reduced tracking time by 45.5% and improved the tracking efficiency by 1.02% [20]. Therefore, the improvements in meta-heuristic algorithms have achieved to reduce power oscillations and present an attractive tracking performance in MPPT compared to basic meta-heuristic algorithms [42].

This study improves GWO to increase MPP tracking speed and efficiency. MPP can be found in a shorter time if the convergence factor is determined according to the proximity

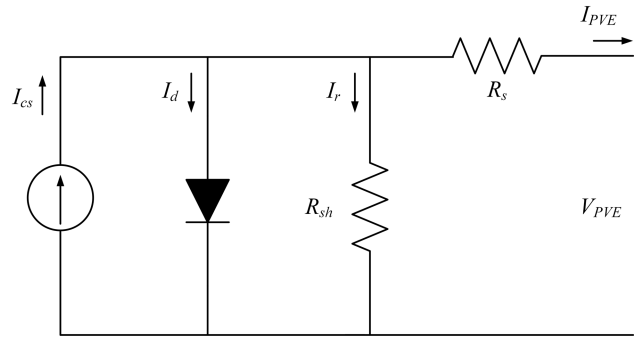

FIGURE 2. Equivalent circuit PVE with a single diode photovoltaic panel.

of α wolves. The other wolves approach the alpha wolf faster, as much as the alpha wolf is closer to the prey. In addition, critical regions have been identified according to the power changes in wolves while hunting. Finally, the results show that the GWO has been improved in terms of global searching-ability, convergence speed, and precision.

The original contributions of this paper are as follows:

- A novel global MPPT method based on an improved GWO is proposed to enhance tracking performance and efficiency.
- Verifications were carried out experimentally using various cases under uniform and non-uniform weather conditions.
- The proposed method provides up to 76% less runtime and up to 2.3% better energy harvesting compared to basic grey wolf optimization, according to the daily performance evaluation under real weather conditions.
- Simple, correct, and helpful PV models are designed using De Soto for PV developers.

The remainder of the paper is organized as follows. Section II explains the study's methodology, including the design stages of PV models and PV emulator (PVE). In addition, the implementation and improvement of GWO are introduced. Section III gives the results of experimental performance evaluations. Section IV concludes the study.

II. METHODOLOGY

PVE equations are provided using a single-diode equivalent circuit of a photovoltaic panel. PV models are introduced using a single-diode equivalent circuit that acts as a PV emulator. Then, shading patterns are described. accordingly, PVMs are generated. After implementing GWO for MPPT, GWO has been improved.

A. DESIGNING PV MODELS AND CHARACTERISTICS OF THE PV EMULATOR

PV model (PVM) simulates characteristic curves of PV arrays in any weather conditions. There are numerous PVM based on the equivalent circuits of single-diode and two-diode [43], [44], [45], [46]. Additionally, PVM based on a three-diode equivalent circuit better shows the losses, but it is quite complex due to nine unknown parameters. PVM parameters

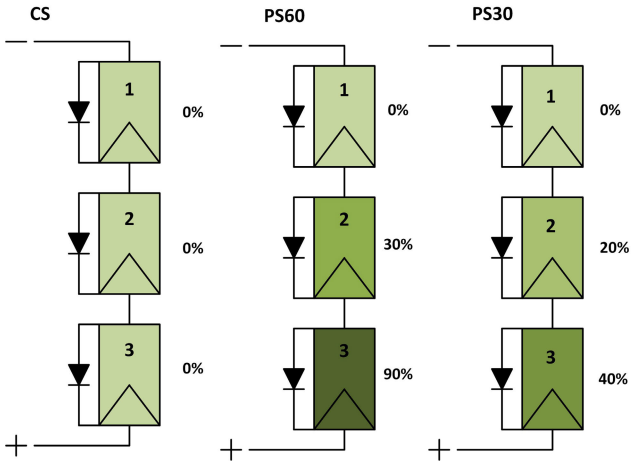

FIGURE 3. Uniform and non-uniform irradiance patterns.

are determined using different optimization algorithms [47], [48], [49]. The PV equivalent circuit in Figure 3 is used to design theoretical PVM. The PV equivalent circuit can be mathematically modeled using Equations 1-5 after calculating the parameters using polynomial equations [50].

$$I_{PV} = I_{ph} - I_d - I_r \tag{1}$$

$$I_{ph} = I_{sho}\left(\frac{S}{1000}\right) + J_0(T - T_{ref}) \tag{2}$$

$$I_d = I_0\left[exp\left(\frac{q(V_{PV} + R_s I_{PV})}{nkT}\right) - 1\right] \tag{3}$$

$$I_0 = I_{d0}\left(\frac{T}{T_{ref}}\right)^3 exp\left(\frac{qE_g}{nk}\left(\frac{1}{T_{ref}} - \frac{1}{T}\right)\right) \tag{4}$$

$$I_r = \frac{(V_{PV} + R_s I_{PV})}{R_{sh}} \tag{5}$$

I_{PV}, I_r, I_d, I_{ph}, and I_0 are currents of PV panel, the shunt resistance, the diode, generated by irradiance, and the reverse saturation diode, respectively. I_{d0}, I_{sho} and J_0 represent reverse diode current, short-circuit current, and temperature coefficient. S is the solar radiation in W/m^2, T_{ref} is the reference temperature at 298 °K, T is the PV cell temperature, E_g is the energy band gap of the cell semiconductor, k is the Boltzmann constant, n is the diode emission factor. R_s and R_{sh} are series and shunt resistances, respectively.

The mathematical models of the PVE with a single PV panel are described in Equation 6-9. PVE acts as a current source generating I_{CS}. The PVE can simulate various I-V curves within the allowed range of equipment with the ability to repeat tests regardless of the atmospheric conditions.

$$I_{PVE} = I_{cs} - I_d - I_r \tag{6}$$

$$I_d = I_0\left[exp\left(\frac{V_{PVE} - R_s I_{PVE}}{N_s V_t}\right) - 1\right] - I_r \tag{7}$$

$$V_{PVE} = I_{PVE}R_s + N_s V_t \ln\left(\frac{I_{PVE} - I_r}{I_0}\right) \tag{8}$$

$$I_r = \frac{V_{PVE} - R_s I_{PVE}}{R_s} \tag{9}$$

PVM, developed by De Soto, is used in the python development environment PVLIB [51] due to its success and ease of use. However, the PVM of PVLIB-De Soto is valid if the series arrays operate under equal radiation. The PS of one of the series-connected arrays significantly reduces the array current. Bypass diodes remove the array under PS from the system until shading passes to prevent the series current from falling [52]. Therefore, the total power of the PV array decreases according to the shading rate. The characteristic curve of the arrays is distorted by the formation of local maximum power points (LMPP) due to PS. There is a need for a second PVM that can reflect PS. Therefore, a new PS model was created by combining PVLIB-De Soto with 0.8 V_{oc} PVMs [53], [54]. During the calculation of the main current passing through the series-connected modules in 0.8 V_{oc} PVM, the voltages of the module V_{sub1} and V_{sub2} were calculated using Equations 10 and 11, considering the change in the radiation level. In the new PS model created by modifying the PVLIB-De Soto PVM; First, three modules connected in series were calculated separately with PVLIB-De Soto PVM. Then, P-V and I-V characteristic curves for PS were created by combining the currents through the first module at voltage V_{sub1}, the second module at V_{sub2}, and the third module at a higher voltage than V_{sub2}. G_1, G_2, G_3 are irradiance levels of PV module. N_1, N_2 are the number of PV array receiving the corresponding irradiation. V_{oc} is the open-circuit voltage. A is a coefficient usually taken as 0.6347.

$$V_{sub1} = N_1 \left[V_{oc} + \frac{1}{A} ln\left(1 - \frac{G_2}{G_1}\right)\right] \tag{10}$$

$$V_{sub2} = V_{sub1} + N_2 \left[V_{oc} + \frac{1}{A} ln\left(1 - \frac{G_3}{G_2}\right)\right] \tag{11}$$

B. INTRODUCING SHADING PATTERNS

The received solar irradiation under clear sky (CS), PS60, and PS30 conditions are given in Figure 4. It is assumed that all three modules receive uniform irradiation under CS. On the other hand, the shading percentages of the three modules under PS60 are 0%, 30%, and 90% of the reference irradiance, and 0%, 20%, and 40% of the reference irradiance under PS30.

C. GENERATING PVM CHARACTERISTICS

The P-V and I-V characteristics of PVMs under standard test conditions (STC) 1000 W/m^2 and 25°C are given in Figure 5. Then, the same P-V and I-V characteristics of PVMs were generated for nine cases which consists of the combinations of different radiations and shading patterns.

The P-V and I-V characteristics of CS, PS60, and PS30 were generated under different irradiation of 1000, 600, and 400 W/m^2 as given in Figure 6. Due to the partial shading, the I-V curves are shaped like staircases. The stars indicate all MPPs in Figure 6. However, only one yellow star represents the GMPP. The rest represents LMPPs that cause power losses due to PS, as indicated with black

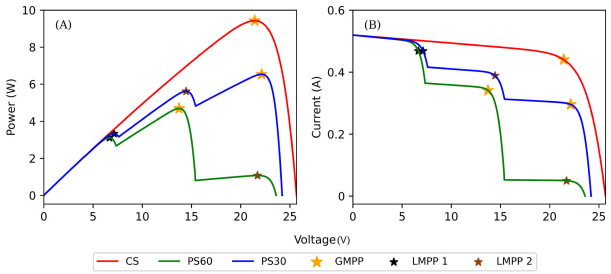

FIGURE 4. a) P-V and b) I-V characteristics of PVMs at STC.

and brown stars in Figure 6.B1, B2 and Figure 6.C1, C2. It is evident in Figure 6.A1 that MPPs were found near the same voltage, whereas the current belonging to MPP changes significantly depending on the radiation. Therefore, the array output power varies under different radiations. Due to partial shading, LMPPs have the lowest current and highest voltage and vice versa, as evident in Figure 6.B2. On the other hand, the slightly differentiated current values have appeared in Figure 6.C2 due to approximate shading percentages. Also, the maximum powers found at GMPP are 9.43, 5.56, and 3.64 W under uniform irradiation of 1000, 600, and 400 W/m^2, respectively. Due to uniform irradiance, there is no local MPP in Cases 1-3. Besides, the irradiance variations under uniform conditions cause up to 4% voltage variation at GMPP (V_{GMPP}). Due to non-uniform irradiance, there exist two LMPPs in Cases 4-9. For example, the P-V characteristics in Case 4-6 of PS60 have two LMPPs at the lower voltage (V_{LMPP_1}) of 6.6 V and higher voltage (V_{LMPP_2}) of 21 V than (V_{GMPP}), which is about 13.5 V. On the contrary, due to different partial shading patterns in Case 7-9 of PS30, the GMPP has been found at the highest voltage of 22 V, whereas LMPPs have been found at lower than (V_{GMPP}). Partial shading patterns significantly affect the location of the GMPP. Table 1 presents the numerical results behind Figure 6.

D. IMPLEMENTING THE GWO FOR MPPT

The GWO algorithm imitates the leadership hierarchy and hunting mechanism of grey wolves in nature. The grey wolf population is divided hierarchically into four categories: alpha (α), beta (β), delta (δ), and omega (ω). α wolf is considered the fittest function. The second and third best solutions are selected β and δ wolves, respectively. ω wolves are assumed to form the remaining candidate solutions. It is seen in Figure 6 that the grey wolves hunt as a group in a certain order. Firstly, they track, pursue, and encircle the prey. Secondly, they irritate the prey until it stops. Finally, they attack the prey.

Equations 12-19 are the mathematical formulation of grey wolves' positions continuously updated during hunting. In Equations 12 and 13, $\vec{A}$ and $\vec{C}$ calculated using the random numbers r_1 and r_2 varying in the range (0, 1), and the regularly decreasing number a starting from 2 and going

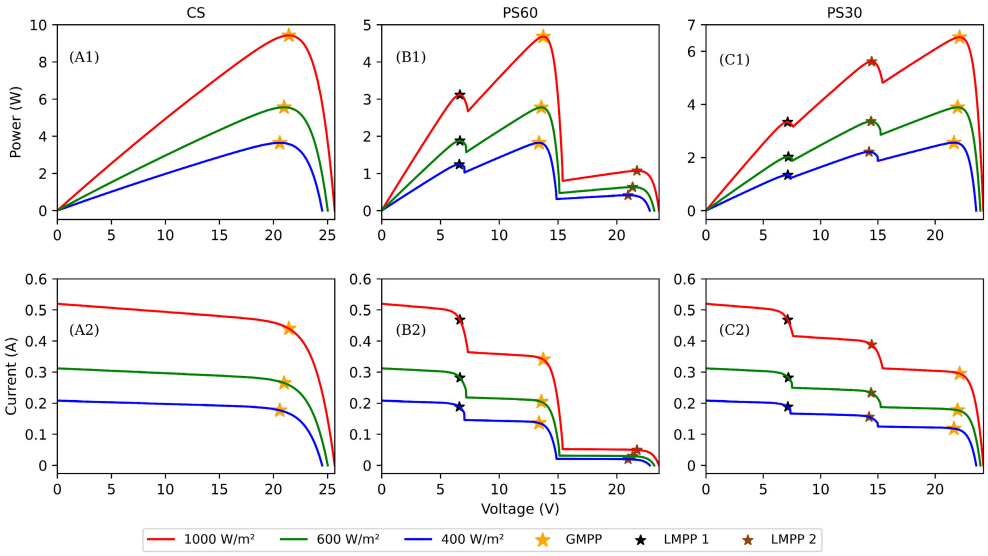

FIGURE 5. P-V and I-V characteristics of PVMs under a) CS, b) PS60 and c) PS30.

TABLE 1. Characteristic results of PVMs.

Pattern	Case	Irradiance (W/m²) Modules (1-2-3)	P_{GMPP} (W)	V_{GMPP} (V)	P_{LMPP_1} (W)	V_{LMPP_1} (V)	P_{LMPP_2} (W)	V_{LMPP_2} (V)
CS	1	1000-1000-1000	9.43	21.42	—	—	—	—
	2	600-600-600	5.56	20.97	—	—	—	—
	3	400-400-400	3.64	20.58	—	—	—	—
PS60	4	1000-700-100	4.68	13.74	3.12	6.66	1.07	21.71
	5	600-420-60	2.78	13.57	1.88	6.66	0.63	21.33
	6	400-280-40	1.82	13.38	1.24	6.61	0.41	20.95
PS30	7	1000-1000-1000	6.53	22.13	3.33	7.12	5.61	14.46
	8	600-480-360	3.89	21.95	2.02	7.18	3.36	14.40
	9	400-320-240	2.56	21.64	1.34	7.14	2.21	14.22

FIGURE 6. Hunting of Grey wolves [55]: A)-B)-C) Tracking, pursuing, encircling the prey, D) Irritating, E) Attacking.

to zero in the last iteration is given.

$$\vec{A} = 2\vec{a} \cdot \vec{r_1} - \vec{a} \tag{12}$$

$$\vec{C} = 2\vec{r_2} \tag{13}$$

In Equations 14 and 15, $\vec{X}_\alpha$, $\vec{X}_\beta$, and $\vec{X}_\delta$ represent the locations of α, β, and δ wolves, respectively. $\vec{X}$ indicates the location of the wolf, and $\vec{D}$ denotes the distance vector of a wolf from prey. Equation 16 determines the next position of the wolf.

$$\begin{aligned} \vec{D}_\alpha &= |\vec{C}_1 \cdot \vec{X}_\alpha - \vec{X}| \\ \vec{D}_\beta &= |\vec{C}_2 \cdot \vec{X}_\beta - \vec{X}| \\ \vec{D}_\delta &= |\vec{C}_3 \cdot \vec{X}_\delta - \vec{X}| \end{aligned} \tag{14}$$

$$\begin{aligned} \vec{X}_1 &= \vec{X}_\alpha - \vec{A}_1 \cdot \vec{D}_\alpha \\ \vec{X}_2 &= \vec{X}_\beta - \vec{A}_2 \cdot \vec{D}_\beta \\ \vec{X}_3 &= \vec{X}_\delta - \vec{A}_3 \cdot \vec{D}_\delta \end{aligned} \tag{15}$$

$$\vec{X}_{(t+1)} = \frac{\vec{X}_1 + \vec{X}_2 + \vec{X}_3}{3} \tag{16}$$

For applying GWO to MPPT, all solutions are considered as the duty cycle of the dc-dc converter (dc), and the position of α wolf is considered the fittest function. The prey is considered the duty cycle corresponding to the GMPP. The

positions of ω wolves are the rest of the possible solutions. Therefore, Equations 14-16 can be modified to Equations 17-19 as follows:

$$\begin{aligned}
\overrightarrow{D}_\alpha &= |\overrightarrow{C}_1 \cdot \overrightarrow{dc}_\alpha - \overrightarrow{dc}| \\
\overrightarrow{D}_\beta &= |\overrightarrow{C}_2 \cdot \overrightarrow{dc}_\beta - \overrightarrow{dc}| \\
\overrightarrow{D}_\delta &= |\overrightarrow{C}_3 \cdot \overrightarrow{dc}_\delta - \overrightarrow{dc}|
\end{aligned} \tag{17}$$

$$\begin{aligned}
\overrightarrow{dc}_1 &= \overrightarrow{dc}_\alpha - \overrightarrow{A}_1 \cdot \overrightarrow{D}_\alpha \\
\overrightarrow{dc}_2 &= \overrightarrow{dc}_\beta - \overrightarrow{A}_2 \cdot \overrightarrow{D}_\beta \\
\overrightarrow{dc}_3 &= \overrightarrow{dc}_\delta - \overrightarrow{A}_3 \cdot \overrightarrow{D}_\delta
\end{aligned} \tag{18}$$

$$\overrightarrow{dc}_{(t+1)} = \frac{\overrightarrow{dc}_1 + \overrightarrow{dc}_2 + \overrightarrow{dc}_3}{3} \tag{19}$$

E. IMPROVING THE GWO ALGORITHM

In this study, GWO was improved to increase speed and efficiency according to the flowchart seen in Figure 8. In the GWO algorithm, grey wolves approach α wolf by narrowing the hunting circle at each iteration with the constant velocity, a_c, which is given in Equation 20. Encircling the prey with constant velocity takes a longer time. If a_c is determined by the degree of closeness of α wolf, the prey can be attacked in a shorter time. If the alpha wolf is closer to the prey, the other wolves approach the alpha wolf faster. However, if the distance between α wolves increases, a is calculated by decreasing a_c. In Equation 21, P_{α_i} and P_r represent the power of the α wolf in iteration "i" and the power difference of the wolves between iterations, respectively. The a_c is calculated using Equation 22 starting from two. As a result of the tests, critical regions for a_c and Δ a steps improving the algorithm performance were determined in Equation 23. The breakpoints of the critical regions P_{r_1} and P_{r_2} were determined to be 0.05 and 0.8, respectively. If Δa is too small, the GWO may lose diversity, and the search process can become trapped in local optima. On the other hand, if Δa is too large, the exploration capability will be high, but the exploitation power will be limited, leading to slower convergence. Therefore, Δa is taken as 0.2 or 0 according to P_r.

$$\overrightarrow{a} = 2 - i\left(\frac{a_c}{i_n}\right) \tag{20}$$

$$P_r = |P_{\alpha_{i+1}} - P_{\alpha_i}| \tag{21}$$

$$a_{c_{(i+1)}} = \begin{cases} a_{c_{(i)}} + \Delta a, P_r < P_{\alpha_i}.P_{r1} \\ a_{c_{(i)}} - \Delta a, P_r > P_{\alpha_i}.P_{r2} \end{cases} \tag{22}$$

$$\Delta a = \begin{cases} 0.2, & \begin{cases} P_r < P_{r1} \\ P_r > P_{r2} \end{cases} \\ 0.0, & P_{r1} < P_r < P_{r2} \end{cases} \tag{23}$$

III. EXPERIMENTAL PERFORMANCE EVALUATIONS

Performing highly accurate tests for MPPT under various radiations and temperatures requires all tests to be carried out under equal conditions [56]. Nevertheless, tests in the open air cannot be in the same weather conditions. Therefore, different methods are required to equalize weather conditions to verify the result of different algorithms under the same condition. For example, different MPPTs can be tested simultaneously using the same experimental setup for each algorithm case. However, it requires as much hardware as the number of test cases [57]. On the other hand, an artificial lighting system that controls radiation and temperature externally was developed to test MPPT under equal conditions [58]. However, the high installation cost and time requirement are the disadvantages of artificial lighting. Therefore, PVE has been developed [59]. PVE is superior to artificial lighting in terms of cost, accuracy, complexity, sensitivity to environmental conditions, and efficiency [60]. Detailed reviews on PVE may be found in [61] and [62]. The PVE

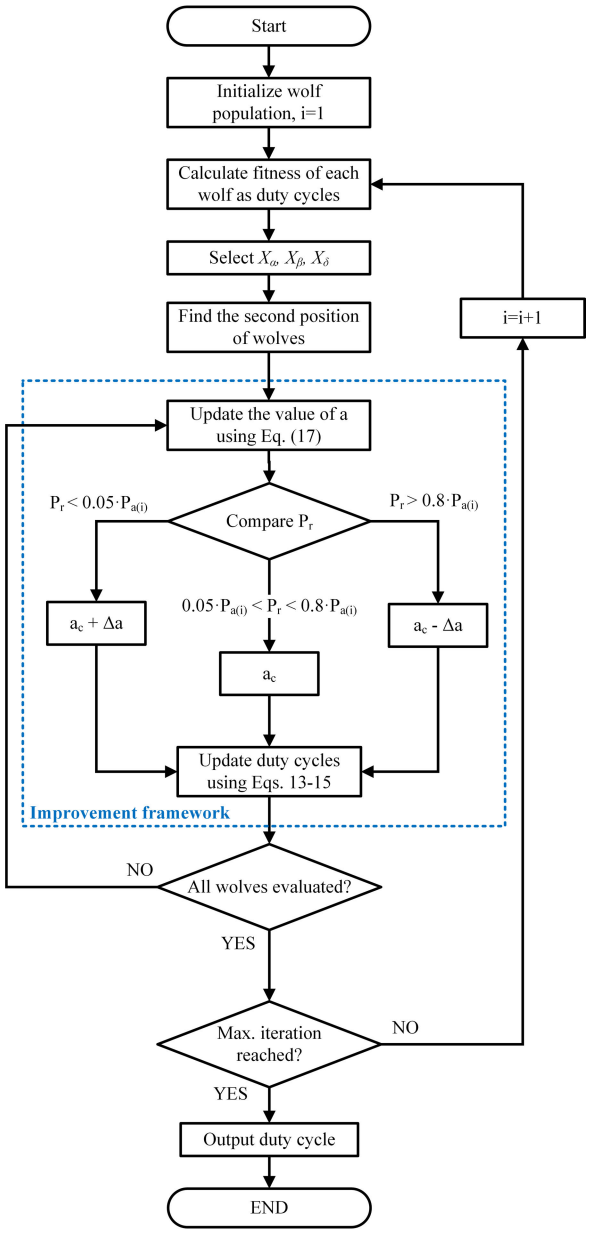

FIGURE 7. Improved GWO flowchart.

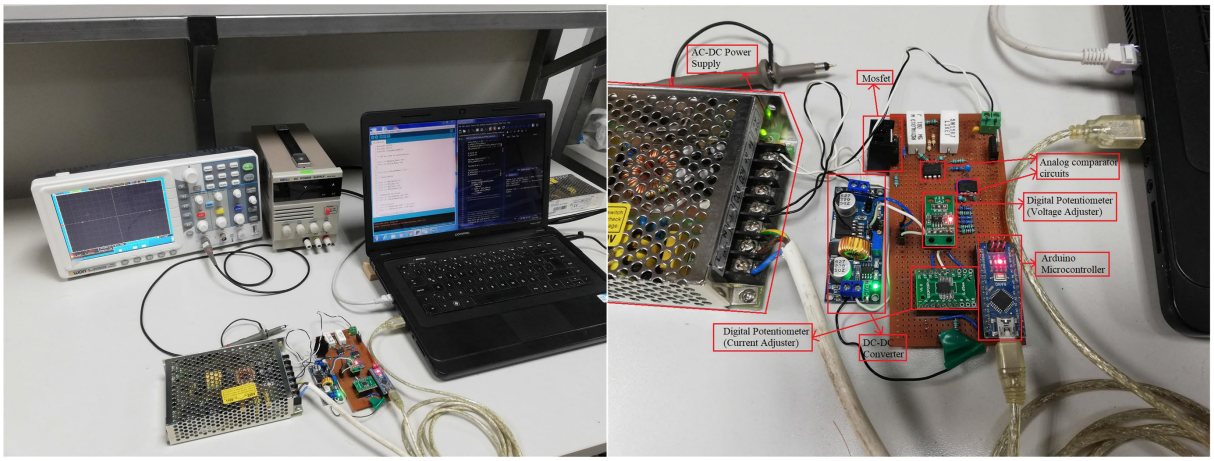

FIGURE 8. Experimental setup.

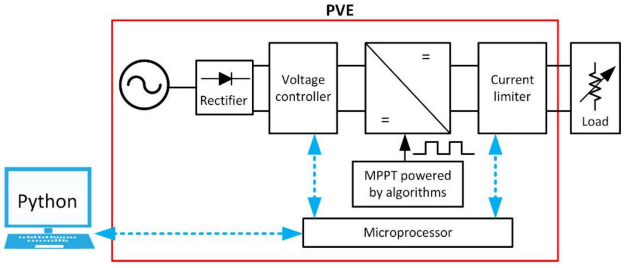

FIGURE 9. The block diagram for proposed global MPPT.

structure communicates with Python as shown in Figure 9. The PV array and weather data selected by the user are entered into the PVLIB-De Soto PVM. The microcontroller controls the current limiting and voltage regulation circuits with an algorithm executed in a Python environment. Then, reference values calculated according to PVM were measured at the DC-DC converter output with approximately 1% RMS error (under standard test conditions) using digital potentiometers. The voltage regulator and current adjuster are set by the digital potentiometer, X9C103 [63], having a resistor array composed of 99 resistive elements and a wiper-switching network. In this way, the success of the optimization algorithms developed in Python in different weather conditions can be compared by running PVE under equal conditions. Figure 9 shows the experimental setup.

A. DYNAMIC TRACKING PERFORMANCE

To verify the tracking ability of the improved GWO (IGWO) based GMPPT method, the dynamic tracking performance of algorithms was experimentally compared under irradiance variations. The irradiance sequence consists of K - L - M stages. Meta-heuristic optimization algorithms were performed in 60 iterations with five search agents using three different PVMs under different radiations. P&O also was performed using 150 steps. Irradiance patterns for dynamic tracking experiments are determined in Table 2.

The power, voltage, and current for the three modules under CS and PS are shown in Figure 10. All algorithms

TABLE 2. Irradiance patterns for dynamic tracking experiments.

Stage	Solar Irradiance (W/m²)	Module	Shading (%)		
			CS	PS60	PS30
K	400	1	0	0	0
		2	0	30	20
		3	0	90	40
L	1000	1	0	0	0
		2	0	30	20
		3	0	90	40
M	600	1	0	0	0
		2	0	30	20
		3	0	90	40

have achieved tracking GMPP under CS. When the irradiance pattern is changed, GWO locates the GMPP of 4.36 W, HHO tracks the GMPP of 4.65 W, and PSO tracks the GMPP of 4.66 W. The P&O works well under uniform radiation conditions, but it is slow in tracking speed and causes power oscillation under partial shading conditions. P&O algorithm is unable to differentiate between LMPP and GMPP. Because it tracks the MPP by constantly changing the terminal voltage of the PV array, it results in steady-state oscillations raising the power loss and reducing the tracking efficiency. The tracking efficiency is calculated as the ratio between the average output power obtained at steady-state and the maximum available power of the PV array under a certain shading pattern. It is evident in Figure 10.A2 and Figure 10.A3 that P&O fails to reach GMPP and gets settled at LMPP of 3.06 W and 3.29 W under PS60 and PS30, and the efficiency reduces by 33% and 47%, respectively.

Meta-heuristic algorithms have higher efficiency under both CS and PS. However, their tracking time and performance differ depending on the nature of the algorithm, especially under PS. For example, HHO has two times more tracking time than other algorithms due to intensely complex operations. Tracking time is used to describe the time it takes to reach a certain convergence condition. Also, the efficiency of PSO and GWO algorithms was reduced by 3.5% and 3% under PS30, respectively. Despite the high tracking time, HHO achieved the best performance, with 99.69% under CS.

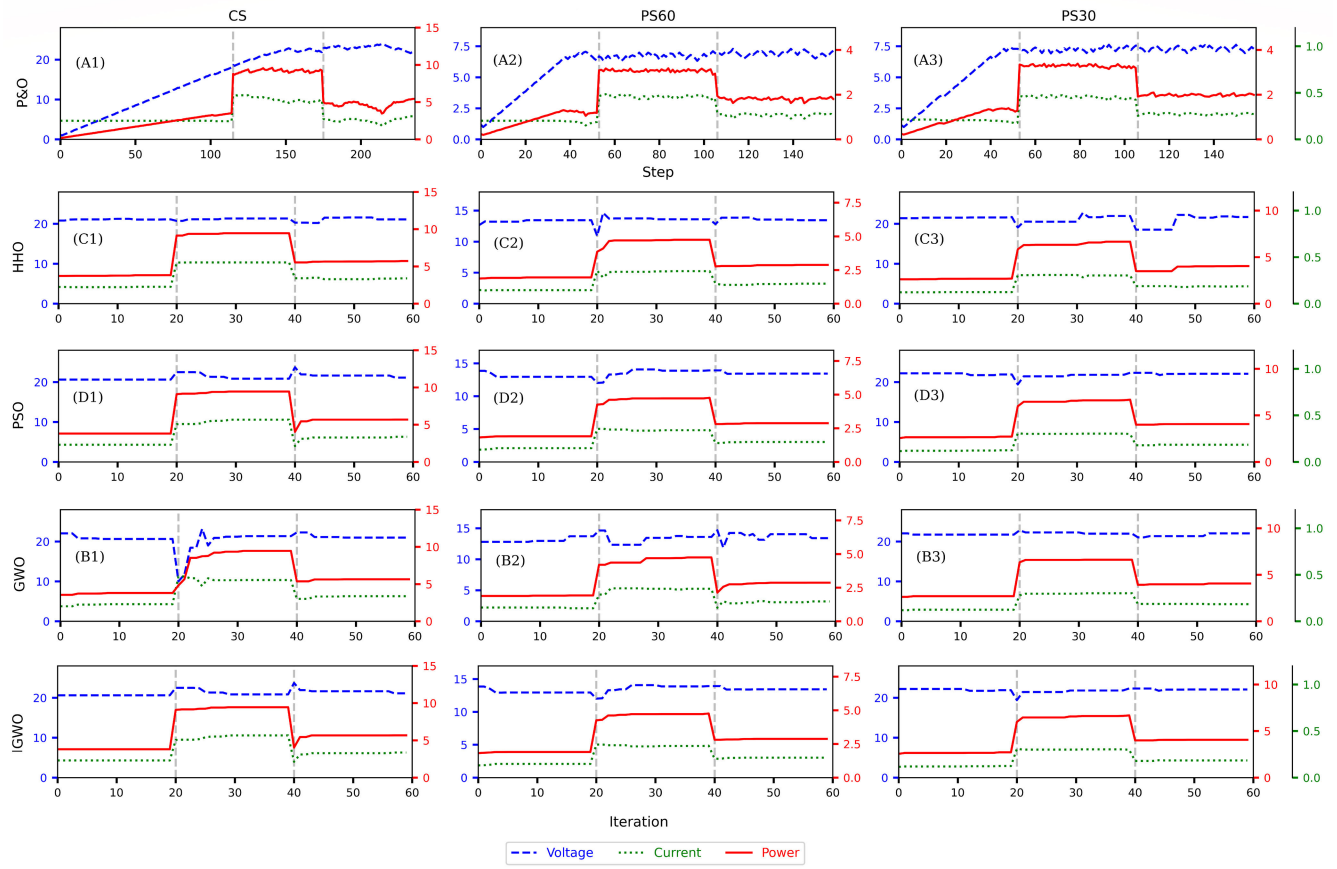

FIGURE 10. Dynamic tracking performance of algorithms.

GWO and PSO have similar tracking times. However, the efficiencies of GWO under PS60 and PS30 were reduced by 2.5% and 0.5%, respectively. PSO is the most suitable MPPT method for PVE due to its higher efficiency and shorter tracking time than traditional meta-heuristic methods. Dynamic tracking performance details such as reference and maximum power, efficiency, and tracking time according to the K, L and M stages are given in Table 3.

On the other hand, according to the dynamic tracking results, the proposed IGWO has improved dynamic tracking speed by up to 82% and increased efficiency by 1.4% compared to the basic GWO. The proposed IGWO has better tracking time and efficiency compared to the study in [20]. Another study improving GWO for MPPT algorithm under partial shading conditions has achieved 58% better tracking speed [64]. The dynamic tracking performance of meta-heuristic algorithms is compared in Figure 11. The IGWO tracks much faster than all other algorithms. Moreover, it has been determined that the proposed IGWO has up to 5 times lower tracking time than PSO.

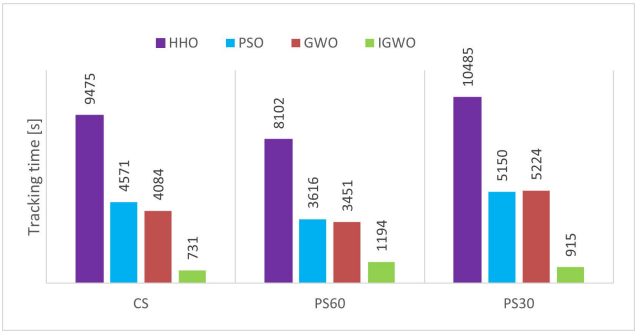

FIGURE 11. Dynamic tracking performance comparison.

B. DAILY PERFORMANCE UNDER REAL WEATHER

The daily performances of algorithms were experimentally compared using measured weather data. The radiation and temperature data were obtained for model simulation and verification using the 15-minute averages of the measured data at the Department of Electrical Engineering of YTU. Figure 12 shows the effects of weather and optimization algorithms on energy harvesting performance for a one-day simulation. The red line represents the observed power, and the dotted blue line represents the theoretical reference power. The daily harvested energies and efficiencies of algorithms under CS are quite similar, with only a 2% difference. The harvested energies in meta-heuristic algorithms of GWO, HHO, and PSO under PS60 and PS30 are less than 50% and 30% compared to CS. On the other hand, the daily harvested energies in P&O under PS60 and PS30 are less than 66% and 62% compared to CS. An extra

TABLE 3. Numerical results of dynamic tracking performance.

Method	PVM	Ref. Power (W)			Max. Power (W)			Efficiency (%)			Avg. Eff. (%)	Tracking time (s)			Total tracking time (s)
		K	L	M	K	L	M	K	L	M		K	L	M	
P&O	CS	3.64	9.43	5.56	3.54	9.33	5.48	97.33	98.93	98.56	98.28	20	49	79	148
	PS60	1.82	4.68	2.78	1.21	3.06	1.79	66.42	65.39	64.28	65.36	14	37	60	111
	PS30	2.56	6.52	3.89	1.28	3.29	2.03	49.99	50.49	52.25	50.91	15	42	64	121
HHO	CS	3.64	9.43	5.56	3.64	9.37	5.54	100	99.38	99.70	99.69	3227	3582	2666	9475
	PS60	1.82	4.68	2.78	1.82	4.65	2.76	100	99.30	99.51	99.60	2908	2483	2711	8102
	PS30	2.56	6.52	3.89	2.56	6.44	3.49	100	98.67	89.66	96.11	3675	3519	3291	10485
PSO	CS	3.64	9.43	5.56	3.64	9.39	5.44	100	99.63	97.89	99.17	1459	1552	1560	4571
	PS60	1.82	4.68	2.78	1.81	4.66	2.78	99.53	99.66	100	99.73	1088	1166	1362	3616
	PS30	2.56	6.52	3.89	2.55	6.46	3.89	99.87	98.95	100	99.61	1595	1770	1785	5150
GWO	CS	3.64	9.43	5.56	3.55	9.34	5.37	97.52	99.11	96.61	97.75	1320	1368	1396	4084
	PS60	1.82	4.68	2.78	1.82	4.36	2.74	100	93.20	98.77	97.32	1077	1226	1148	3451
	PS30	2.56	6.52	3.89	2.56	6.34	3.89	100	97.10	100	99.03	1670	1816	1738	5224
IGWO	CS	3.64	9.43	5.56	3.63	9.32	5.56	99.68	98.86	100	99.51	121	142	468	731
	PS60	1.82	4.68	2.78	1.80	4.68	2.78	98.78	99.93	100	99.57	489	349	356	1194
	PS30	2.56	6.52	3.89	2.56	6.52	3.79	100	100	97.47	99.16	72	410	433	915

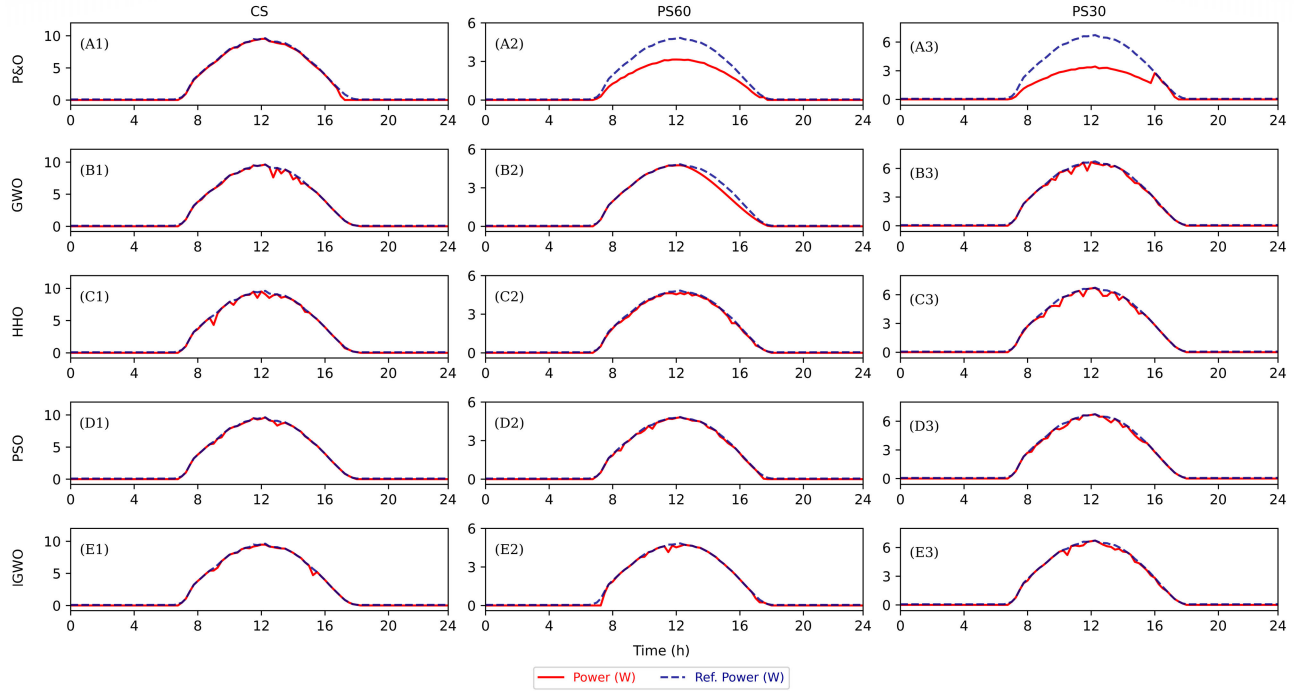

FIGURE 12. Daily performance of meta-heuristic algorithms.

energy loss is observed during non-uniform irradiance conditions because the gradient nature of P&O leads to falling into LMPP.

Moreover, it is evident in Figure 12.E2 that the IGWO resolves the observed power deviation in Figure 12.B2. HHO shows weak performance in average efficiency and tracking time among the other meta-heuristic algorithms. Under CS, the IGWO reduces the runtime of GWO because of the ability to narrow down the search area. Runtime comparison reveals that the GWO took 2075 s while the IGWO took 1962.77 s under PS60. However, the GWO completes over 8000 s and the IGWO completes in 1947.5 s under PS30. Thus, IGWO is an average of 4 times faster than GWO under PS30. Consequently, the runtime comparison reveals that partial shading conditions affect the performance of algorithms. Therefore, the IGWO has up to 76% better tracking performance than GWO, according to the daily performance evaluation under real weather conditions. On the other hand, the daily performance of IGWO has similar efficiency to PSO, but the IGWO is much faster than PSO. The daily performance of algorithms is compared in Table 4 in terms of daily harvested energy, efficiency, and runtime. Runtime is the time it takes for all iterations to complete. The runtime of meta-heuristic algorithms is presented in Figure 13. The IGWO has a powerful performance among the other meta-heuristic algorithms.

TABLE 4. Comparison of the daily performance of algorithms.

	CS	PS60	PS30	Harvested Energy [Wh/d]	Efficiency [%]	Avg. Efficiency [%]	Runtime (s)
P&O	✓			63.71	97.54	71.94	418.91
		✓		21.84	65.59		237.47
			✓	24.39	52.68		242.66
HHO	✓			63.82	97.66	97.11	14872.00
		✓		32.29	96.98		20652.71
			✓	44.76	96.69		40985.00
PSO	✓			64.63	98.94	98.10	10337.99
		✓		32.61	97.94		19040.57
			✓	45.10	97.42		17545.02
GWO	✓			64.60	98.81	97.92	1303.43
		✓		32.48	97.54		2075.00
			✓	45.10	97.41		8006.28
IGWO	✓			64.61	98.88	98.12	1051.45
		✓		32.62	97.91		1962.77
			✓	45.18	97.58		1947.51

Note: Reference energy values are 65.32 (CS), 33.27 (PS60), 46.3 (PS30) Wh.

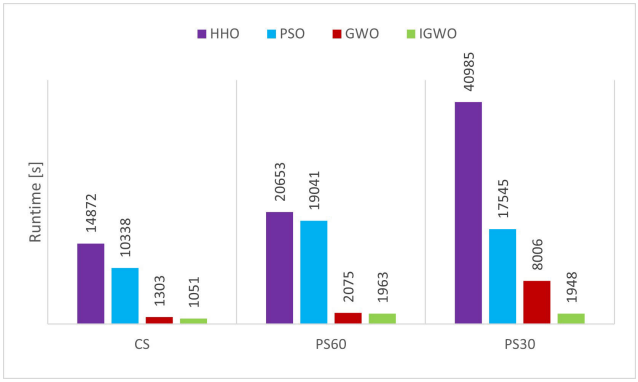

FIGURE 13. Daily runtime comparison of meta-heuristic algorithms.

IV. CONCLUSION AND POTENTIAL FUTURE WORK

This study proposed a novel global MPPT method using the proposed IGWO. Uniform and non-uniform weather conditions were modeled by combining PVLIB-De Soto and 0.8 Voc in a Python environment. Therefore, simple, correct, and helpful PV models are designed for PV developers. The performance of IGWO was compared to several optimization algorithms such as P&O, PSO, HHO, GWO, and IGWO. Dynamic tracking performance of gradient based P&O is faster, but it falls into LMPPs because of partial shading conditions. On the other hand, meta-heuristic algorithms have found GMPP with high efficiency, but they have taken a long time due to the randomness and complexity. Consequently, the IGWO has increased dynamic tracking speed by up to 82% and efficiency by up to 1.4% compared to the basic GWO. The daily performance under real weather conditions has validated the results of dynamic tracking performance. The results revealed that the IGWO performs better than the other meta-heuristic algorithms. Additionally, the IGWO reduces the runtime by up to 76% and improves energy harvesting up to 2.3% more than basic GWO, thanks to narrowing down the search area of GWO. The future research direction will be hybridizing meta-heuristic algorithms with artificial neural networks, helping to design and develop solar PV systems.

REFERENCES

[1] N. Karami, N. Moubayed, and R. Outbib, "General review and classification of different MPPT techniques," *Renew. Sustain. Energy Rev.*, vol. 68, pp. 1–18, Feb. 2017.

[2] S. Sarwar, M. Y. Javed, M. H. Jaffery, J. Arshad, A. U. Rehman, M. Shafiq, and J.-G. Choi, "A novel hybrid MPPT technique to maximize power harvesting from PV system under partial and complex partial shading," *Appl. Sci.*, vol. 12, no. 2, p. 587, Jan. 2022.

[3] M. H. Zafar, N. M. Khan, A. F. Mirza, M. Mansoor, N. Akhtar, M. U. Qadir, N. A. Khan, and S. K. R. Moosavi, "A novel meta-heuristic optimization algorithm based MPPT control technique for PV systems under complex partial shading condition," *Sustain. Energy Technol. Assessments*, vol. 47, Oct. 2021, Art. no. 101367.

[4] M. H. Zafar, N. M. Khan, A. F. Mirza, and M. Mansoor, "Bio-inspired optimization algorithms based maximum power point tracking technique for photovoltaic systems under partial shading and complex partial shading conditions," *J. Cleaner Prod.*, vol. 309, Aug. 2021, Art. no. 127279.

[5] K. M. and J. S., "A novel coarse and fine control algorithm to improve maximum power point tracking (MPPT) efficiency in photovoltaic system," *ISA Trans.*, vol. 121, pp. 180–190, Feb. 2022.

[6] H. Gundogdu and A. Demirc, "Performance comparison of grey wolf and perturb & observe MPPT algorithms in different weather conditions," in *Proc. 13th Int. Conf. Electr. Electron. Eng. (ELECO)*, Nov. 2021, pp. 84–89.

[7] V. Jately, B. Azzopardi, J. Joshi, B. Venkateswaran V, A. Sharma, and S. Arora, "Experimental analysis of hill-climbing MPPT algorithms under low irradiance levels," *Renew. Sustain. Energy Rev.*, vol. 150, Oct. 2021, Art. no. 111467. [Online]. Available: https://www.sciencedirect.com/science/article/pii/S1364032121007498

[8] V. Jately, S. Bhattacharya, B. Azzopardi, A. Montgareuil, J. Joshi, and S. Arora, "Voltage and current reference based MPPT under rapidly changing irradiance and load resistance," *IEEE Trans. Energy Convers.*, vol. 36, no. 3, pp. 2297–2309, Sep. 2021.

[9] S. M. Tercan, A. Demirci, Y. E. Unutmaz, O. Elma, and R. Yumurtaci, "A comprehensive review of recent advances in optimal allocation methods for distributed renewable generation," *IET Renew. Power Gener.*, vol. 17, no. 12, pp. 3133–3150, Sep. 2023.

[10] M. Mao, L. Zhang, H. Huang, B. Chong, and L. Zhou, "Maximum power exploitation for grid-connected PV system under fast-varying solar irradiation levels with modified salp swarm algorithm," *J. Cleaner Prod.*, vol. 268, Sep. 2020, Art. no. 122158.

[11] S. Rajamand, "A novel sliding mode control and modified PSO-modified P&O algorithms for peak power control of PV," *ISA Trans.*, vol. 130, pp. 533–552, Nov. 2022.
[12] S. Javed and K. Ishaque, "A comprehensive analyses with new findings of different PSO variants for MPPT problem under partial shading," *Ain Shams Eng. J.*, vol. 13, no. 5, Sep. 2022, Art. no. 101680.
[13] M. Abdulkadir, A. H. M. Yatim, and S. T. Yusuf, "An improved PSO-based MPPT control strategy for photovoltaic systems," *Int. J. Photoenergy*, vol. 2014, pp. 1–11, Jan. 2014.
[14] I. Dagal and B. Akin, "Improved particle swarm optimization based on buck-boost converter (IPSO-BBC) for photovoltaic system applications," *Recent Adv. Sci. Eng.*, vol. 2, no. 2, pp. 42–48, 2022.
[15] M. H. Qais, H. M. Hasanien, and S. Alghuwainem, "Parameters extraction of three-diode photovoltaic model using computation and Harris hawks optimization," *Energy*, vol. 195, Mar. 2020, Art. no. 117040.
[16] M. Mansoor, A. F. Mirza, and Q. Ling, "Harris hawk optimization-based MPPT control for PV systems under partial shading conditions," *J. Cleaner Prod.*, vol. 274, Nov. 2020, Art. no. 122857.
[17] S. Mirjalili, S. M. Mirjalili, and A. Lewis, "Grey wolf optimizer," *Adv. Eng. Softw.*, vol. 69, pp. 46–61, Mar. 2014.
[18] N. Rawat, P. Thakur, A. K. Singh, A. Bhatt, V. Sangwan, and A. Manivannan, "A new grey wolf optimization-based parameter estimation technique of solar photovoltaic," *Sustain. Energy Technol. Assessments*, vol. 57, Jun. 2023, Art. no. 103240.
[19] S. Mohanty, B. Subudhi, and P. K. Ray, "A new MPPT design using grey wolf optimization technique for photovoltaic system under partial shading conditions," *IEEE Trans. Sustain. Energy*, vol. 7, no. 1, pp. 181–188, Jan. 2016.
[20] I. S. Millah, P. C. Chang, D. F. Teshome, R. K. Subroto, K. L. Lian, and J.-F. Lin, "An enhanced grey wolf optimization algorithm for photovoltaic maximum power point tracking control under partial shading conditions," *IEEE Open J. Ind. Electron. Soc.*, vol. 3, pp. 392–408, 2022.
[21] S. N. Makhadmeh, M. A. Al-Betar, I. A. Doush, M. A. Awadallah, S. Kassaymeh, S. Mirjalili, and R. A. Zitar, "Recent advances in grey wolf optimizer, its versions and applications: Review," *IEEE Access*, early access, 2023, doi: 10.1109/ACCESS.2023.3304889.
[22] L. Gong, G. Hou, and C. Huang, "A two-stage MPPT controller for PV system based on the improved artificial bee colony and simultaneous heat transfer search algorithm," *ISA Trans.*, vol. 132, pp. 428–443, Jan. 2023.
[23] R. S. Pal and V. Mukherjee, "Metaheuristic based comparative MPPT methods for photovoltaic technology under partial shading condition," *Energy*, vol. 212, Dec. 2020, Art. no. 118592.
[24] Z. Pan, N. V. Quynh, Z. M. Ali, S. Dadfar, and T. Kashiwagi, "Enhancement of maximum power point tracking technique based on PV-battery system using hybrid BAT algorithm and fuzzy controller," *J. Cleaner Prod.*, vol. 274, Nov. 2020, Art. no. 123719.
[25] S. Motahhir, A. El Hammoumi, and A. El Ghzizal, "The most used MPPT algorithms: Review and the suitable low-cost embedded board for each algorithm," *J. Cleaner Prod.*, vol. 246, Feb. 2020, Art. no. 118983.
[26] A. Moghassemi, S. Ebrahimi, S. Padmanaban, M. Mitolo, and J. B. Holm-Nielsen, "Two fast metaheuristic-based MPPT techniques for partially shaded photovoltaic system," *Int. J. Electr. Power Energy Syst.*, vol. 137, May 2022, Art. no. 107567.
[27] Z. Xie and Z. Wu, "A flexible power point tracking algorithm for photovoltaic system under partial shading condition," *Sustain. Energy Technol. Assessments*, vol. 49, Feb. 2022, Art. no. 101747.
[28] Y. Jiang, J. Xu, X. Leng, and N. Eghbalian, "A novel hybrid maximum power point tracking method based on improving the effectiveness of different configuration partial shadow," *Sustain. Energy Technol. Assessments*, vol. 50, Mar. 2022, Art. no. 101835.
[29] N. A. Windarko, E. N. Sholikhah, M. N. Habibi, E. Prasetyono, B. Sumantri, M. Z. Efendi, and H. Mokhlis, "Hybrid photovoltaic maximum power point tracking of seagull optimizer and modified perturb and observe for complex partial shading," *Int. J. Electr. Comput. Eng.*, vol. 12, no. 5, p. 4571, Oct. 2022.
[30] S. Mohanty, B. Subudhi, and P. K. Ray, "A grey wolf-assisted perturb & observe MPPT algorithm for a PV system," *IEEE Trans. Energy Convers.*, vol. 32, no. 1, pp. 340–347, Mar. 2017.
[31] J. Ahmed and Z. Salam, "An enhanced adaptive P&O MPPT for fast and efficient tracking under varying environmental conditions," *IEEE Trans. Sustain. Energy*, vol. 9, no. 3, pp. 1487–1496, Jul. 2018.
[32] S. K. T., V. Reddy, and A. Robinson, "An innovative grey wolf optimizer with Nelder–mead search method based MPPT technique for fast convergence under partial shading conditions," *Sustain. Energy Technol. Assessments*, vol. 59, Oct. 2023, Art. no. 103412.
[33] M. H. Nadimi-Shahraki, S. Taghian, and S. Mirjalili, "An improved grey wolf optimizer for solving engineering problems," *Expert Syst. Appl.*, vol. 166, Mar. 2021, Art. no. 113917.
[34] L. Zhang, T. Gao, G. Cai, and K. L. Hai, "Research on electric vehicle charging safety warning model based on back propagation neural network optimized by improved gray wolf algorithm," *J. Energy Storage*, vol. 49, May 2022, Art. no. 104092.
[35] İ. Yazıcı and E. K. Yaylacı, "Modified grey wolf optimizer based MPPT design and experimentally performance evaluations for wind energy systems," *Eng. Sci. Technol., Int. J.*, vol. 46, Oct. 2023, Art. no. 101520.
[36] W. Long, J. Jiao, X. Liang, and M. Tang, "An exploration-enhanced grey wolf optimizer to solve high-dimensional numerical optimization," *Eng. Appl. Artif. Intell.*, vol. 68, pp. 63–80, Feb. 2018.
[37] R. Motamarri, N. Bhookya, and B. Chitti Babu, "Modified grey wolf optimization for global maximum power point tracking under partial shading conditions in photovoltaic system," *Int. J. Circuit Theory Appl.*, vol. 49, no. 7, pp. 1884–1901, Jul. 2021.
[38] Y. Li, X. Lin, and J. Liu, "An improved gray wolf optimization algorithm to solve engineering problems," *Sustainability*, vol. 13, no. 6, p. 3208, Mar. 2021.
[39] S. Saleem, I. Ahmad, S. H. Ahmed, and A. Rehman, "Artificial intelligence based robust nonlinear controllers optimized by improved gray wolf optimization algorithm for plug-in hybrid electric vehicles in grid to vehicle applications," *J. Energy Storage*, vol. 75, Jan. 2024, Art. no. 109332.
[40] Q. Xie, Z. Guo, D. Liu, Z. Chen, Z. Shen, and X. Wang, "Optimization of heliostat field distribution based on improved gray wolf optimization algorithm," *Renew. Energy*, vol. 176, pp. 447–458, Oct. 2021.
[41] K. Guo, L. Cui, M. Mao, L. Zhou, and Q. Zhang, "An improved gray wolf optimizer MPPT algorithm for PV system with BFBIC converter under partial shading," *IEEE Access*, vol. 8, pp. 103476–103490, 2020.
[42] M. Mao, L. Cui, Q. Zhang, K. Guo, L. Zhou, and H. Huang, "Classification and summarization of solar photovoltaic MPPT techniques: A review based on traditional and intelligent control strategies," *Energy Rep.*, vol. 6, pp. 1312–1327, Nov. 2020.
[43] R. Venkateswari and N. Rajasekar, "Review on parameter estimation techniques of solar photovoltaic systems," *Int. Trans. Electr. Energy Syst.*, vol. 31, no. 11, p. e13113, Nov. 2021.
[44] E. Batzelis, "Non-iterative methods for the extraction of the single-diode model parameters of photovoltaic modules: A review and comparative assessment," *Energies*, vol. 12, no. 3, p. 358, Jan. 2019.
[45] B. Maniraj and A. P. Fathima, "Parameter extraction of solar photovoltaic modules using various optimization techniques: A review," *J. Phys., Conf. Ser.*, vol. 1716, no. 1, Dec. 2020, Art. no. 012001.
[46] F. E. Ndi, S. N. Perabi, S. E. Ndjakomo, G. O. Abessolo, and G. M. Mengata, "Estimation of single-diode and two diode solar cell parameters by equilibrium optimizer method," *Energy Rep.*, vol. 7, pp. 4761–4768, Nov. 2021.
[47] M. H. Qais, H. M. Hasanien, and S. Alghuwainem, "Identification of electrical parameters for three-diode photovoltaic model using analytical and sunflower optimization algorithm," *Appl. Energy*, vol. 250, pp. 109–117, Sep. 2019.
[48] O. S. Elazab, H. M. Hasanien, I. Alsaidan, A. Y. Abdelaziz, and S. M. Muyeen, "Parameter estimation of three diode photovoltaic model using grasshopper optimization algorithm," *Energies*, vol. 13, no. 2, p. 497, Jan. 2020.
[49] J. D. Bastidas-Rodriguez, G. Petrone, C. A. Ramos-Paja, and G. Spagnuolo, "A genetic algorithm for identifying the single diode model parameters of a photovoltaic panel," *Math. Comput. Simul.*, vol. 131, pp. 38–54, Jan. 2017.
[50] T. Ikegami, T. Maezono, F. Nakanishi, Y. Yamagata, and K. Ebihara, "Estimation of equivalent circuit parameters of PV module and its application to optimal operation of PV system," *Sol. Energy Mater. Sol. Cells*, vol. 67, nos. 1–4, pp. 389–395, Mar. 2001.
[51] W. F. Holmgren, C. W. Hansen, and M. A. Mikofski, "Pvlib Python: A Python package for modeling solar energy systems," *J. Open Source Softw.*, vol. 3, no. 29, p. 884, Sep. 2018.

[52] H. Patel and V. Agarwal, "MATLAB-based modeling to study the effects of partial shading on PV array characteristics," *IEEE Trans. Energy Convers.*, vol. 23, no. 1, pp. 302–310, Mar. 2008.
[53] J. Ahmed and Z. Salam, "An improved method to predict the position of maximum power point during partial shading for PV arrays," *IEEE Trans. Ind. Informat.*, vol. 11, no. 6, pp. 1378–1387, Dec. 2015.
[54] H. Patel and V. Agarwal, "Maximum power point tracking scheme for PV systems operating under partially shaded conditions," *IEEE Trans. Ind. Electron.*, vol. 55, no. 4, pp. 1689–1698, Apr. 2008.
[55] C. Muro, R. Escobedo, L. Spector, and R. P. Coppinger, "Wolf-pack (Canis lupus) hunting strategies emerge from simple rules in computational simulations," *Behav. Processes*, vol. 88, no. 3, pp. 192–197, Nov. 2011.
[56] A. Chalh, S. Motahhir, A. El Hammoumi, A. El Ghzizal, and A. Derouich, "Study of a low-cost PV emulator for testing MPPT algorithm under fast irradiation and temperature change," *Technol. Econ. Smart Grids Sustain. Energy*, vol. 3, no. 1, p. 11, Dec. 2018.
[57] Z. Zhou, P. M. Holland, and P. Igic, "MPPT algorithm test on a photovoltaic emulating system constructed by a DC power supply and an indoor solar panel," *Energy Convers. Manage.*, vol. 85, pp. 460–469, Sep. 2014.
[58] A. Haque, "Maximum power point tracking (MPPT) scheme for solar photovoltaic system," *Energy Technol. Policy*, vol. 1, no. 1, pp. 115–122, Jan. 2014.
[59] R. Ayop and C. W. Tan, "A comprehensive review on photovoltaic emulator," *Renew. Sustain. Energy Rev.*, vol. 80, pp. 430–452, Dec. 2017.
[60] J. P. Ram, H. Manghani, D. S. Pillai, T. S. Babu, M. Miyatake, and N. Rajasekar, "Analysis on solar PV emulators: A review," *Renew. Sustain. Energy Rev.*, vol. 81, pp. 149–160, Jan. 2018.
[61] M. Shahabuddin, A. Riyaz, M. Asim, M. M. Shadab, A. Sarwar, and A. Anees, "Performance based analysis of solar PV emulators: A review," in *Proc. Int. Conf. Comput. Characterization Techn. Eng. Sci. (CCTES)*, Sep. 2018, pp. 94–99.
[62] Z. Zhou and J. Macaulay, "An emulated PV source based on an unilluminated solar panel and DC power supply," *Energies*, vol. 10, no. 12, p. 2075, Dec. 2017.
[63] Renesas Corporation. (2023). *Digitally Controlled Potentiometer*. Accessed: Dec. 8, 2023. [Online]. Available: https://www.renesas.com/us/en/document/dst/x9c102-x9c103-x9c104-x9c503-datasheet?r=502671
[64] D. J. K. Kishore, M. R. Mohamed, K. Sudhakar, and K. Peddakapu, "An improved grey wolf optimization based MPPT algorithm for photovoltaic systems under diverse partial shading conditions," *J. Phys., Conf. Ser.*, vol. 2312, no. 1, Aug. 2022, Art. no. 012063, doi: 10.1088/1742-6596/2312/1/012063.

HASAN GUNDOGDU received the B.Sc. degree in electrical engineering from Yildiz Technical University, İstanbul, Turkey, in 2021, where he is currently pursuing the M.Sc. degree in electrical machines and power electronics. Since 2021, he has been an Electrical Engineer with the Propulsion Electronic System Team. His research interests include renewable energy systems, electrical machines, power electronics, UAVs, and electrical vehicles. He published several articles related his research areas.

ALPASLAN DEMIRCI received the B.Sc. degree in electrical and electronics engineering from Sakarya University, Turkey, the B.Sc. and M.Sc. degrees in electrical education from Marmara University, İstanbul, Turkey, in 2007 and 2011, respectively, and the Ph.D. degree in electrical engineering from the Graduate School of Science and Engineering, Yildiz Technical University (YTU), İstanbul, in 2023. He is currently an Assistant Professor with the Department of Electrical Engineering, YTU. His research interests include power system optimization methods, distributed renewable energy systems, energy economics, electric vehicles, and energy storage systems. He has published several articles related his research areas.

SAID MIRZA TERCAN received the B.Sc. degree from the Department of Electrical Engineering, Istanbul Technical University, in 2012, and the M.Sc. and Ph.D. degrees in electrical engineering from the Graduate School of Science and Engineering, Yildiz Technical University (YTU), in 2015 and 2022, respectively. He is currently an Assistant Professor with the Department of Electrical Engineering, YTU. His research interests include energy storage systems, power distribution grid, renewable energy systems, and electric vehicles. He has published several articles and conference papers related his research areas.

UMIT CALI received the B.E. degree in electrical engineering from Yildiz Technical University, İstanbul, Turkey, in 2000, and the M.Sc. degree in electrical communication engineering and the Ph.D. degree in electrical engineering and computer science from the University of Kassel, Germany, in 2005 and 2010, respectively. With over 20 years of experience in both industry and academia, he is currently a Professor of Digital Engineering for Future Technologies with the University of York. His research interests include energy informatics, artificial intelligence, blockchain technology, renewable energy systems, and energy economics. He is also the Chair for the Digital Privacy-Energy Industry TC under IEEE Future Directions. He serves as the Vice Chair for the IEEE Blockchain in Energy Standards WG (P2418.5).